ELSEVIER

Thermochimica Acta 282/283 (1996) 13–27

thermochimica acta

The kinetic interpretation of the decomposition of calcium carbonate by use of relationships other than the Arrhenius equation[1]

David Dollimore[a,*], Ping Tong[b], Kenneth S. Alexander[b]

[a] *Department of Chemistry, University of Toledo 2801 W. Bancroft St., Toledo, Ohio 43606–3390, USA*

[b] *College of Pharmacy, University of Toledo 2801 W. Bancroft St., Toledo, Ohio 43606–3390, USA*

Abstract

The kinetic parameters needed to describe the decomposition of calcium carbonate are obtained by a method which avoids the direct use of the Arrhenius parameters, the pre-exponential term A and the energy of activation E. It is shown that the approach is amenable to both an exact differential and integral analysis which carries certain advantages over existing methods. If needed, the method can be extended to allow the calculation of the Arrhenius parameters A and E, and in addition will show any dependence of E upon the fraction decomposed α, although it might be argued that the dependence of E is really upon the temperature..

Keywords: Arrhenius equation; Kinetic; Calcium carbonate; Decomposition

1. Introduction

There is a considerable literature showing deviant behavior when plots are made of the Arrhenius equation [1]. In solid state decomposition kinetics, the most common deviant behavior is two or three linear regions shown in the plot of log(rate constant) against reciprocal temperature in degrees Kelvin. In some cases a continuous curve may be obtained which can be considered as an infinite collection of linear regions.

* Corresponding author.

[1] Dedicated to Takeo Ozawa on the Occasion of his 65th Birthday.

PII S0040-6031(95)02810-9

The logarithmic relation between the specific reaction rate (k) and the temperature (T) in degrees Kelvin was first recorded by Hood [2] as

$$\log k = \frac{A'}{T} + \text{constant} \tag{1}$$

where A' is also a constant. Arrhenius [3] restated the relationship given by Eq. (1) as

$$\ln k = -\frac{E}{RT} + \ln A \tag{2}$$

or

$$k = A\mathrm{e}^{-E/RT} \tag{3}$$

The analogy with the Van't Hoff relationship is obvious. In eqs. (2) and (3), A is the pre-exponential factor and E is the activation energy necessary for a reaction to occur. R is the gas constant. An alternative equation was put forward by Harcourt and Esson [4], namely

$$k = CT^{\mathrm{m}} \tag{4}$$

where C is a constant and m is also a positive constant.

In solid state reactions, the concept of concentration is meaningless, so the extent of reaction, or the fraction decomposed and designated as α, is used and has values from 0 to 1. There are various models, usually based on geometric factors, or diffusion or both [5] which are designated in Table 1. The specific reaction rate is then defined as

$$\frac{\mathrm{d}\alpha}{\mathrm{d}t} = kf(\alpha) \tag{5}$$

where t is the time and $f(\alpha)$ some function of α [6]. As already there are many instances where the kinetic data for solid state decomposition when plotted according to the Arrhenius equation gives two or more linear regions or even a continuous curve [7, 8]. It would seem inappropriate to base an analysis of increasing temperature data on a single Arrhenius equation unless more data were available.

2. Theory

In non-isothermal kinetic studies the usual method of analysis is simply to utilize three relationships. The first is to relate the temperature (T) with the rate of heating (b)

$$T = T_0 + bt \tag{6}$$

where T_0 is the starting temperature. Combining this with the kinetic expression Eq. (5) will lead to

$$\frac{\mathrm{d}\alpha}{\mathrm{d}T} = \frac{\mathrm{d}\alpha}{\mathrm{d}t} \times \frac{\mathrm{d}t}{\mathrm{d}T} = \frac{kf(\alpha)}{b} \tag{7}$$

Table 1
Classification of mathematical expressions of reaction mechanisms

	Kinetic classification	$g(\alpha)=\int\frac{d\alpha}{f(\alpha)}=kt$	$f(\alpha)=\frac{1}{k}\left(\frac{d\alpha}{dt}\right)$
(1) *Acceleratory* α–t *curves*			
P_1	Power law	$\alpha^{1/n}$	$n(\alpha)^{(n-1)/n}$
E_1	Exponential law	$\ln\alpha$	α
(2) *Sigmoidal* α–t *curves*			
A_2	Avrami–Erofeev	$[-\ln(1-\alpha)]^{1/2}$	$2(1-\alpha)[-\ln(1-\alpha)]^{1/2}$
A_3	Avrami–Erofeev	$[-\ln(1-\alpha)]^{1/3}$	$3(1-\alpha)[-\ln(1-\alpha)]^{2/3}$
A_4	Avrami–Erofeev	$[-\ln(1-\alpha)]^{1/4}$	$4(1-\alpha)[-\ln(1-\alpha)]^{3/4}$
B_1	Prout–Tompkins	$\ln[\alpha/(1-\alpha)]+C$	$\alpha(1-\alpha)$
(3) *Deceleratory* α–t *curves*			
(3.1) Based on geometrical models			
R2	Contracting area	$1-(1-\alpha)^{1/2}$	$2(1-\alpha)^{1/2}$
R3	Contracting volume	$1-(1-\alpha)^{1/3}$	$3(1-\alpha)^{2/3}$
(3.2) Based on diffusion mechanisms			
D1	One-dimensional	α^2	$\frac{1}{2}\alpha$
D2	Two-dimensional	$(1-\alpha)\ln(1-\alpha)+\alpha$	$[-\ln(1-\alpha)]^{-1}$
D3	Three-dimensional	$[1-(1-\alpha)^{1/3}]^2$	$\frac{3}{2}(1-\alpha)^{2/3}[1-(1-\alpha)^{1/3}]^{-1}$
D4	Ginstling–Brounshtein	$(1-2\alpha/3)-(1-\alpha)^{2/3}$	$\frac{3}{2}[(1-\alpha)^{-1/3}-1]^{-1}$
(3.3) Based on "order" of reaction			
F1	First-order	$-\ln(1-\alpha)$	$1-\alpha$
F2	Second-order	$(1-\alpha)^{-1}$	$(1-\alpha)^2$
F3	Third-order	$[(1-\alpha)]^{-2}$	$\frac{1}{2}(1-\alpha)^3$

or

$$k=\frac{\left(\frac{d\alpha}{dT}\right)b}{f(\alpha)} \tag{8}$$

If the Arrhenius equation is assumed, then from Eqs. (2) and (8), it follows that

$$\ln\left(\frac{\left(\frac{d\alpha}{dT}\right)b}{f(\alpha)}\right)=\ln A-\frac{E}{RT} \tag{9}$$

A plot of $\ln(((d\alpha/dT)b)/f(\alpha))$ against $1/T$ should then allow the calculation of A and E. This approach is termed the Arrhenius differential method.

Rearrangement and integration provides the equation

$$g(\alpha)=\int_0^{\alpha}\frac{d\alpha}{f(\alpha)}=\frac{A}{b}\int_{T_i}^{T}e^{-E/RT}dT \tag{10}$$

where T_i is the initial temperature of the reaction and T the temperature in the reaction zone concerned. The analysis of kinetic data using this equation is known as the integral method. The term $\int e^{-E/RT} dT$ does not provide an analytical solution so alternative approximation methods have been used in the application of Eq. (10) [9–12].

A simpler approach is to replace the Arrhenius equation by the Harcourt and Esson relationship (Eq. (4)). In this application there is also a differential equation and an integrated equation. In the use of the integrated equation, however, there is no need for approximation methods. The Harcourt and Esson differential approach is to put Eq. (4) into log form

$$\log k = \log C + m \log T \tag{11}$$

or

$$\log \frac{\left(\frac{d\alpha}{dT}\right) b}{f(\alpha)} = \log C + m \log T \tag{12}$$

A plot of $\log (((d\alpha/dT)b)/f(\alpha))$ against $\log T$ allows the calculation of m from the slope and C from the intercept. The choice of function α ($F(\alpha)$, see Table 1) is discussed latter in this article. The Harcourt and Esson integral approach is achieved by rearrangement of Eq. (4) to give

$$\frac{\left(\frac{d\alpha}{dT}\right) b}{f(\alpha)} = C T^m \tag{13}$$

and then integration to give

$$g(\alpha) = \int_0^{\alpha} \frac{d\alpha}{f(\alpha)} = \frac{C}{b} \int_{T_i}^{T} T^m dT \tag{14}$$

This can be written:

$$g(\alpha) = \frac{C}{b} \frac{T^{m+1}}{m+1} + D \tag{15}$$

where $g(\alpha) = \int_0^{\alpha} (d\alpha/f(\alpha))$ (see Table 1), and D is a constant of integration. This can be written simply as

$$g(\alpha) = B T^{m+1} + D \tag{16}$$

where $B = C/b(m+1)$. This approach is called the integral method. When T is significantly large, then D will be comparatively small and negligible. Taking logarithms on both sides of Eq. (16) gives

$$\log (g(\alpha)) = \log B + (m+1) \log T \tag{17}$$

from which m can be calculated from the slope of the plot of log $(g(\alpha))$ against log T. The treatment of this equation is taken further when considering the experimental data. A plot of $g(\alpha)$ against T^{m+1} will substantiate the approach outlined here.

To make this general approach reasonable, there has to be a method of selecting the appropriate kinetic expression, so that the correct form of $f(\alpha)$ and $g(\alpha)$ can be used. The models upon which these experiments are based have been reviewed by Brown et al. [5] and the most commonly used of these are listed in Table 1. The choice can be narrowed down from these 15 expressions by considering the shape of the TG plot or other thermal analysis signals from which the α–T plot can be derived. Dollimore and coworkers [13–18] have shown that the mechanism can be determined by a consideration of the following parameters.

(i) Judging the character of the initial reaction temperature (T_i) as diffuse T_i(d) or sharp T_i(s) and with similar designations for the final reaction temperature (T_f) as T_f(d) or T_f(s). (Fig. 1A).

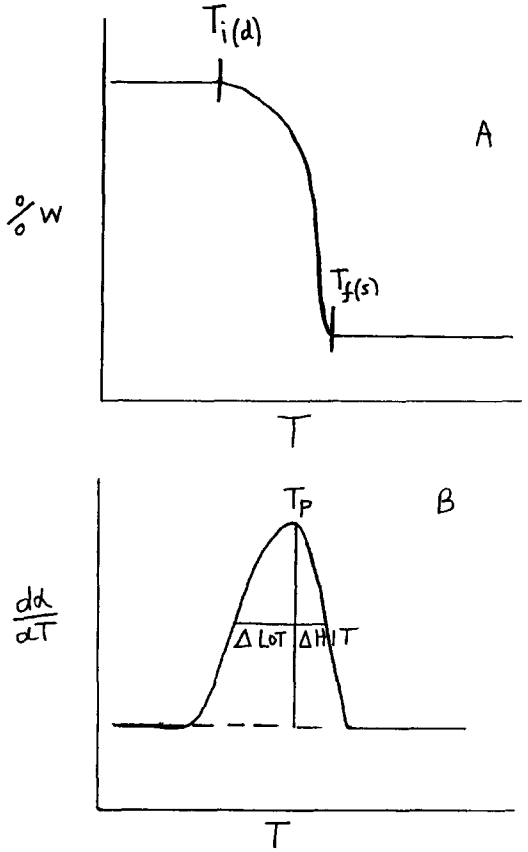

Fig. 1. Schematic representation showing characteristic parameters for determining reaction mechanism. A. Typical TGA plot showing T_i diffuse and T_f sharp. B. Typical DTG plot showing half-width. C. Typical α–T plot showing α_{max} at T_p.

(ii) The half-width, defined as the width on the differential plot of $(d\alpha/dT)$ against T measured at the half-way point of the line drawn from the peak temperature perpendicular to the base line which is drawn between the initial temperature (T_i) and the final temperature (T_f). For clarity this is shown schematically in Fig. 1B.

(iii) α_{max} — this is the value of α at the maximum rate of decomposition (at T_p) for the $\alpha-T$ plot under consideration.

It has been shown that a separation by virtue of the above parameters will enable a kinetic mechanism to be identified or, at worst, will narrow the choice down to two or three mechanisms. It is possible to adopt various schemes involving the above parameters and such a scheme is presented in Table 2 and in the flowchart in Table 3.

Table 2
Characterization of kinetic mechanisms based on the shape of TG plots

Group	Mechanisms	Characteristic features of T_i and T_f	$\Delta LoT^a/\Delta HiT$
A	A_2, A_3, A_4	T_i sharp, T_f sharp	≈ 1
B	R_2, R_3, D_1, D_2, D_3, D_4	T_i diffuse, T_f sharp	$\gg 1$
C	F_1, F_2, F_3	T_i diffuse, T_f diffuse	≈ 1

[a] Ratio at the half-width of low and high temperature tails of the derivative peak (see Fig. 1B).

Table 3
Flow chart showing the procedures in recognizing the kinetic mechanisms

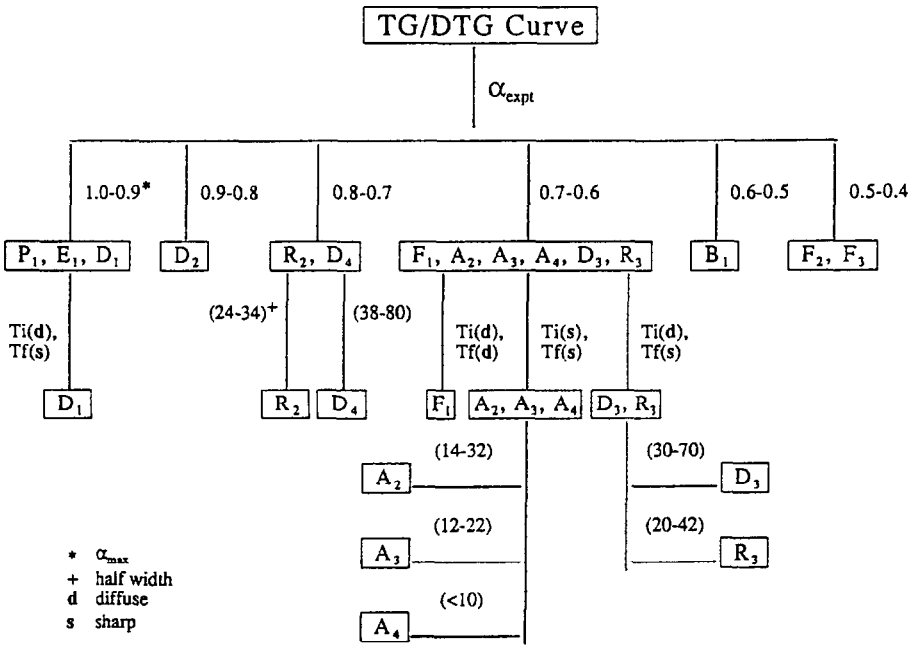

3. Experimental

3.1. Materials

The calcium carbonate used in this study is a Fisher scientific product (Lot No. CAS-471-34-1). In some experiments it was diluted by addition of colloidal silicon dioxide which had the effect of separating the particles. The silica used was amorphous fumed silica (Grade M-5, Lot No. 1E252).

3.2. Technique

A simultaneous TGA and DTA unit (TA SDT 2960) was used in the present study. The heating rate was 10°C min^{-1}, and the experiments were carried out in a flowing atmosphere of dry nitrogen (flow rate 50 ml min^{-1}). The sample cells were platinum crucibles. The sample mass was 10–25 mg. The reference cell was left empty.

The mixing of calcium carbonate with colloidal silica in different ratios (1:0.2, 1:0.5 and 1:1) was done by grinding the mixture in a mortar.

4. Results and discussion

The TGA/DTG curve of calcium carbonate is shown in Fig. 2. The same material was subjected to TG runs after being diluted with colloidal silica at different ratios

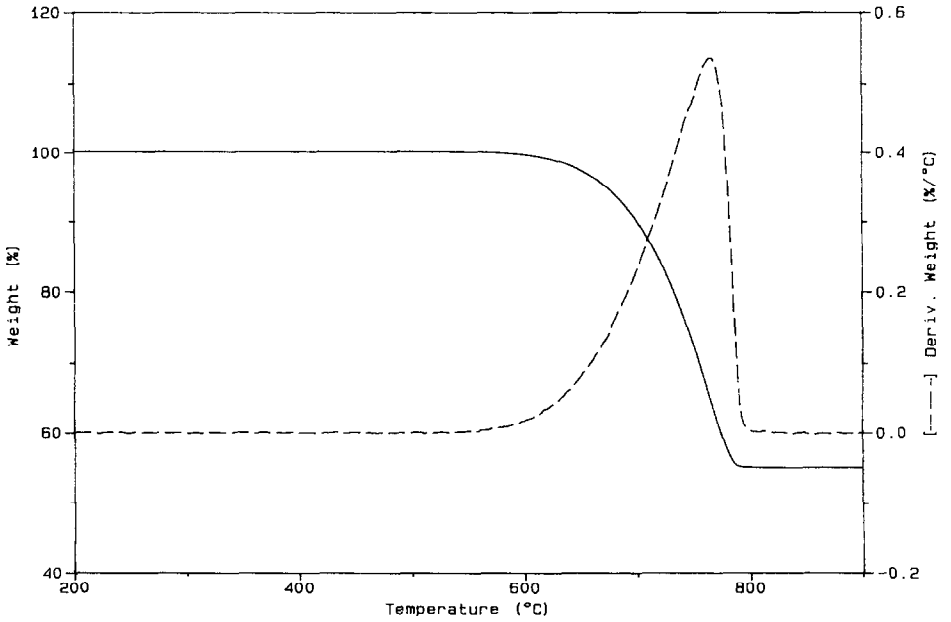

Fig. 2. TGA/DTG curve for calcium carbonate.

($CaCO_3$: silica, 1 : 0, 1 : 0.2, 1 : 0.5 and 1 : 1). Then each sample was heated in a domestic microwave for 10 min, and then subjected to TG runs again. All the runs were perfomed in a dry nitrogen atmosphere. The data are reduced to comparative plots of α against T before and after different treatments, as shown in Figs. 3 and 4, respectively.

4.1. Recognizing the kinetic mechanisms

It has been shown that quantitative information including peak temperature (T_p), (α_{max}), ((ΔLoT)/(ΔHiT)) and half-width may serve as indicators of the most probable rate equation and thus pinpoint, or at least narrow down, the possible decomposition mechanism.

According to Table 4, all the TG plots show (T_i) diffuse and (T_f) sharp, and ((ΔLoT)/(ΔHiT)) > 1 indicating that all the decompositions belong to group B, which includes mechanisms R_2, R_3, D_1, D_2, D_3 and D_4. Following the flowchart (Table 3), all the experimental (α_{max}) values fall between 0.768 and 0.810, implying that R_2 and D_4 are the possible mechanisms.

When the half-width is taken into consideration, D_4 is favored over R_2 since all the half widths are around 80. Although the half-width of many runs falls beyond 80, this

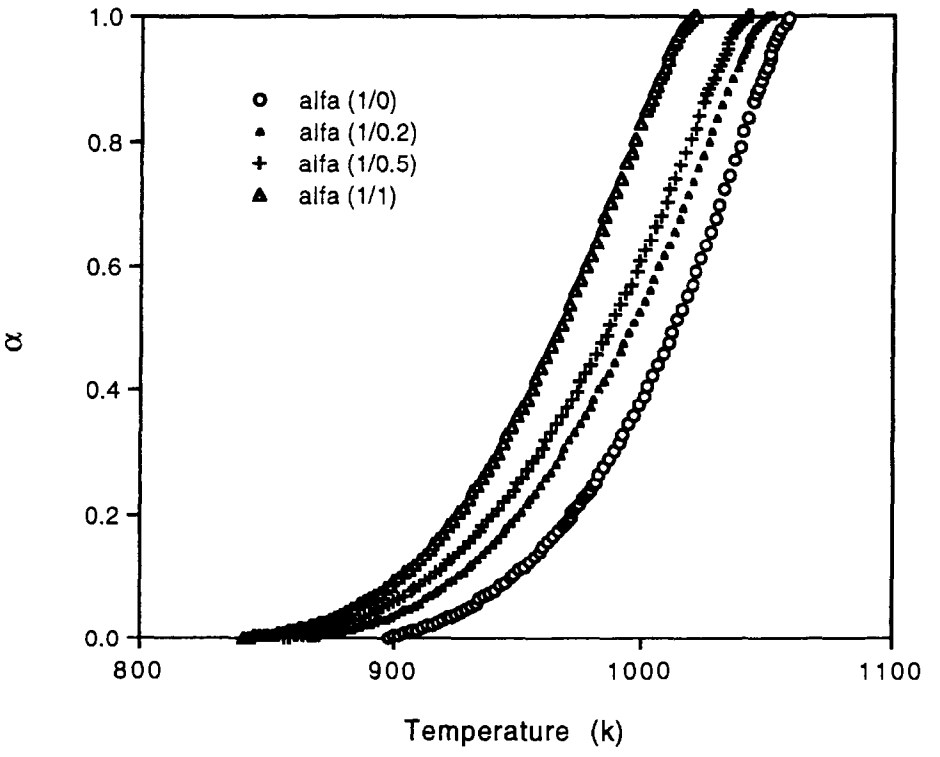

Fig. 3. Comparative α–T plots for $CaCO_3$ before and after addition of colloidal silica in different ratios.

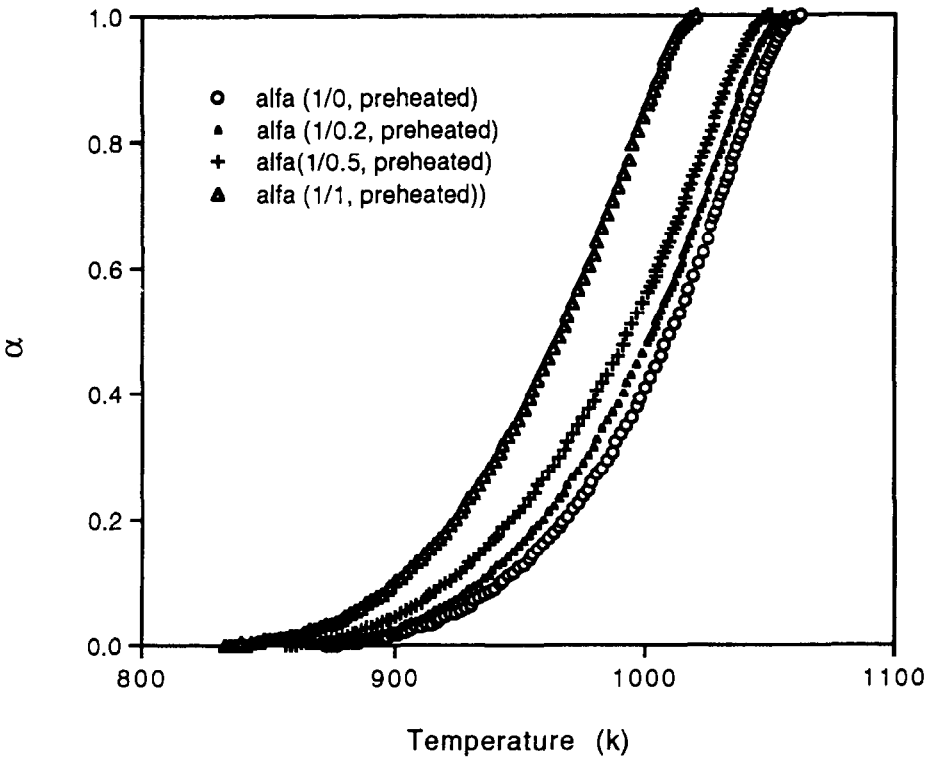

Fig. 4. Comparative α–T plots for mixtures of $CaCO_3$/colloidal silica of different ratios before and after microwave preheating treatment.

Table 4
Parameters pertaining to mechanism-characteristic features for the decomposition of $CaCO_3$ after different treatments

Sample no.	Treatment[a]	T_p/°C	T_i/T_f shape	$\Delta LoT/\Delta HiT$	α_{max}	Half-width/°C
1	1:0.0	766.8	d/s	3.417	0.799	73.77
2	1:0.2	754.8	d/s	4.163	0.798	86.07
3	1:0.5	747.6	d/s	4.351	0.792	87.70
4	1:1.0	723.6	d/s	4.042	0.717	83.67
5	1:0.0(h)	764.4	d/s	3.417	0.803	77.45
6	1:0.2(h)	759.6	d/s	4.163	0.789	77.87
7	1:0.5(h)	752.4	d/s	4.351	0.775	81.97
8	1:1.0(h)	721.2	d/s	4.042	0.768	81.96

[a] The ratios represent that the binary mixture of calcium carbonate and silica; h stands for preheating treatment.

deviation, as well as the fact that α_{max} values fluctuate around 0.8, is believed to be the result of a broad DTG peak.

Therefore, D_4 was taken as the possible mechanism. This was based on the appropriate kinetic expressions for $f(\alpha)$ and $g(\alpha)$ obtained from Table 1. The Arrhenius and Harcourt–Esson relationships, utilizing both the differential and integral methods, were used to calculate the Arrhenius parameters A and E.

4.2. *Effect of colloidal silica and preheating on kinetic parameters*

A typical Arrhenius differential plot ($\ln k$ against $1/T$) is given in Fig. 5. A typical Harcourt–Esson differential plot ($\ln k$ against $\log T$) is shown in Fig. 6; alternatively, the Harcourt–Esson integral method in the form of Eq. (16) is applied by plotting $\log(g(\alpha))$ against $\log T$, as seen in Fig. 7.

Kinetic parameters for all three relationships are summarized in Table 5. It is seen that the terms A, E, m and C showed a gradual alteration with the different treatments of calcium carbonate. With the addition of silica, the TG and DTG plots shifted toward the left, indicating a decreasing trend in peak temperature with an increase in the ratio of silica. The Arrhenius parameters A and E also showed the same decreasing trend with the addition of silica. The preheating, however, showed little effect on the kinetic

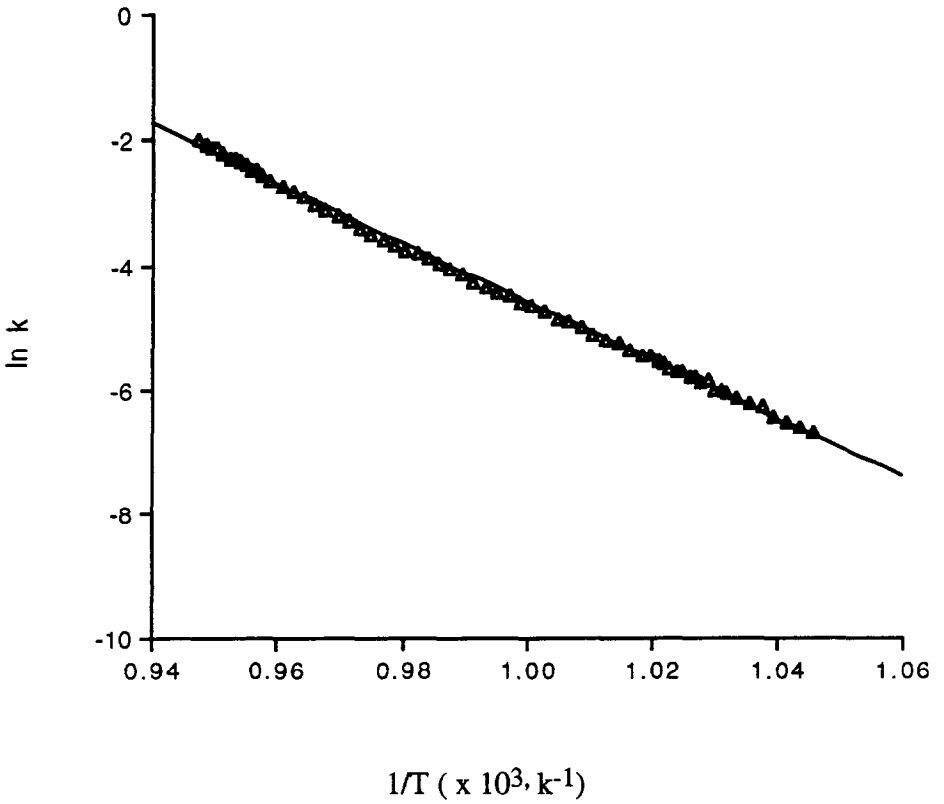

Fig. 5. Typical plot of a differential form of the Arrhenius relationship (data from sample 1).

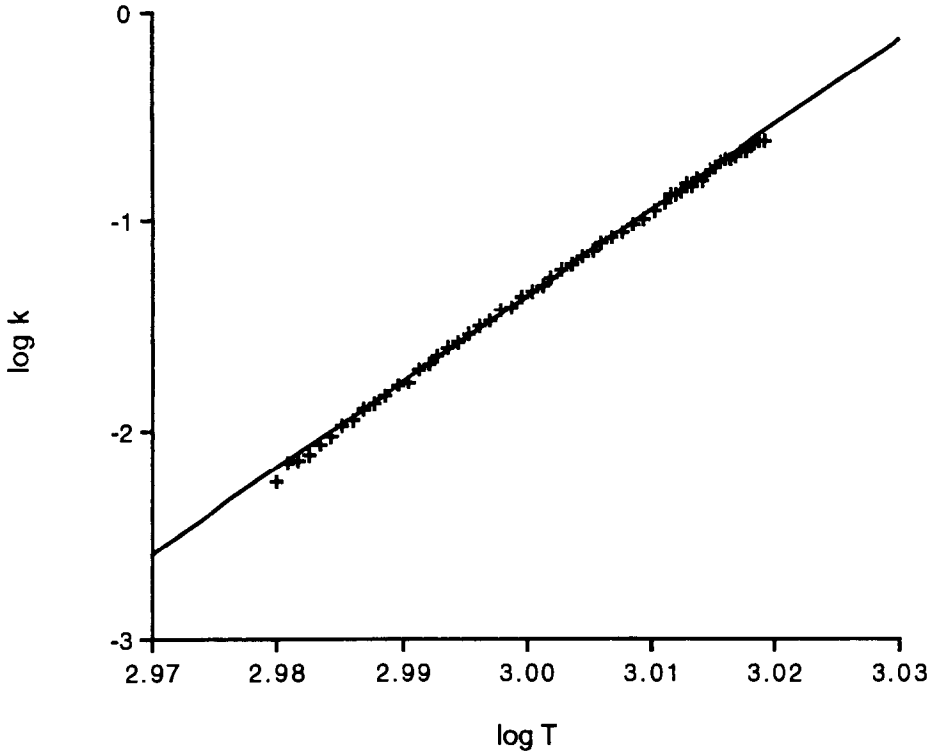

Fig. 6. Typical plot of a differential form of the Harcourt and Essent relationship (data from sample 5).

behavior of calcium carbonate. The alterations for samples 7, 8 and 9 were caused mainly by the addition of silica.

The D_4 mechanism is based on a modification of a three-dimensional diffusion out of a sphere derived by Ginstling and Brounshtein [19]. Therefore, the reactions are governed by diffusion. In solid state decomposition, the most common method of dealing with a structure change is to explain these changes on the basis of nucleation followed by the advance of reaction interface in which the changes are taking place. The alternative is to assume a homogeneous process distributed throughout the volume of the solid reactant [20]. In both cases, the concept of nucleation, nucleation growth and the advance of the reaction interface is dominant [21].

It is likely that silica acts as a "spacer", causing fewer points of contact between particles of calcium carbonate. This has the effect of increasing the interface of calcium carbonate which allows more chances of formation of nucleation. Haul and Stein [22] identified two steps for the diffusion for calcium carbonate decomposition: a rapid initial diffusion confined to a surface layer and a slow diffusion process within the lattice. They also found that the surface diffusion is favored over the diffusion within the lattice. Thus, the surface area may become significant in describing the kinetic behavior.

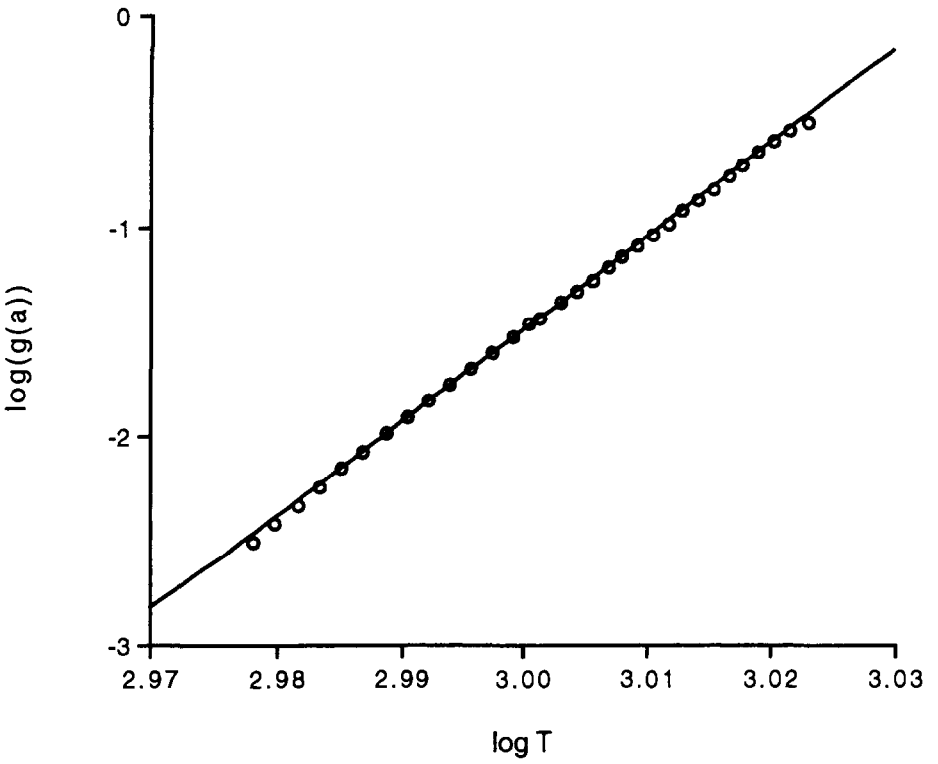

Fig. 7. Typical plot of an integral form of the Harcourt and Esson relationship (data from sample 6).

Table 5
Kinetic parameters obtained from different methods

Sample no.	E/kJ mol^{-1} (A – D)[a]	A (A – D)	m		C	
			(H&E – D)	(H&E – I)	(H&E – D)	(H&E – I)
1	391	2.74×10^{18}	46.75	47.99	6×10^{-143}	1×10^{-146}
2	327	2.47×10^{15}	39.81	40.54	7×10^{-122}	4×10^{-124}
3	318	1.08×10^{15}	38.14	37.01	1×10^{-116}	8×10^{-113}
4	319	2.95×10^{15}	38.99	41.15	6×10^{-119}	2×10^{-125}
5	373	3.44×10^{17}	44.16	45.42	4×10^{-135}	5×10^{-139}
6	359	8.35×10^{16}	42.02	43.56	1×10^{-128}	2×10^{-133}
7	322	1.42×10^{15}	39.34	40.56	2×10^{-120}	4×10^{-124}
8	328	2.88×10^{16}	40.68	41.40	6×10^{-124}	3×10^{-126}

[a] A – D is Arrhenius differential method; H&D-D is Harcourt and Esson differential method; H&D-I is Harcourt and Esson integral method.

4.3. Dependence of activation energy on α or temperature

In the application of the Harcourt and Esson relationship, if the Arrhenius parameters A and E are required, this can be achieved by using the relationship at specific temperatures. Thus at temperature T_1

$$k(T_1) = CT_1^m = Ae^{-E/RT_1} \tag{18}$$

and at temperature T_2

$$k(T_2) = CT_2^m = Ae^{-E/RT_2} \tag{19}$$

When the temperature increment is as small as 2°C, the temperature-dependent rate constant k and activation energy E can be regarded as the same at T_1 and T_2, thus

$$\left(\frac{T_2}{T_1}\right)^m = \frac{e^{-E/RT_2}}{e^{-E/RT_1}} = e^{E\Delta T/RT_1T_2} \tag{20}$$

Taking the logarithm on both sides gives

$$m(\ln T_2 - \ln T_1) = \frac{E\Delta T}{RT_1T_2} \tag{21}$$

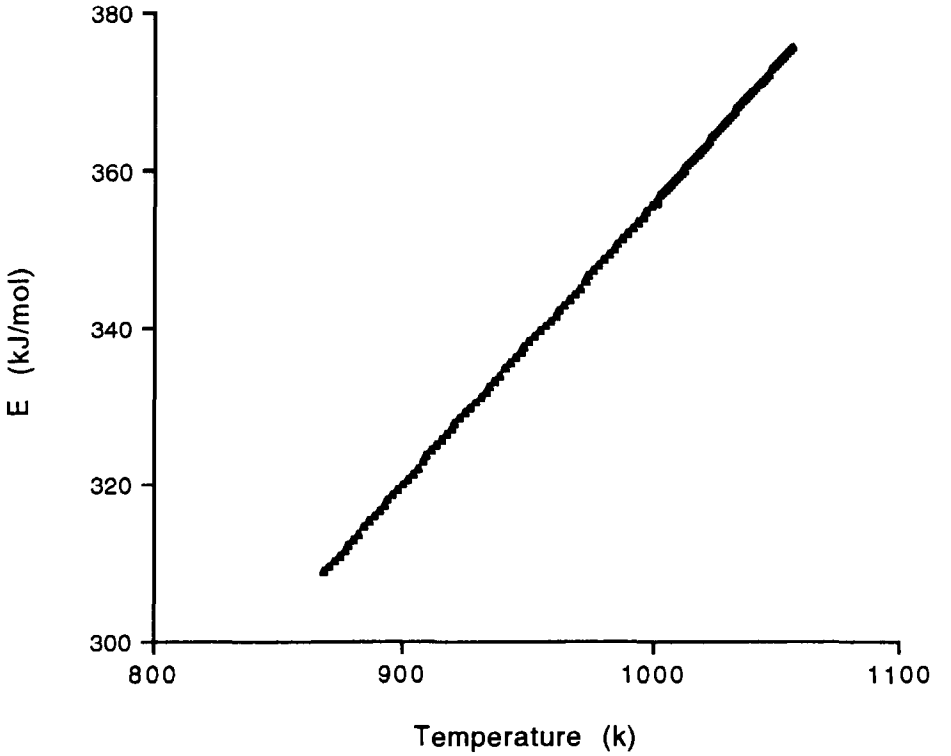

Fig. 8. Plot of E against temperature in Kelvin taken from the mid-point of the ΔT increment.

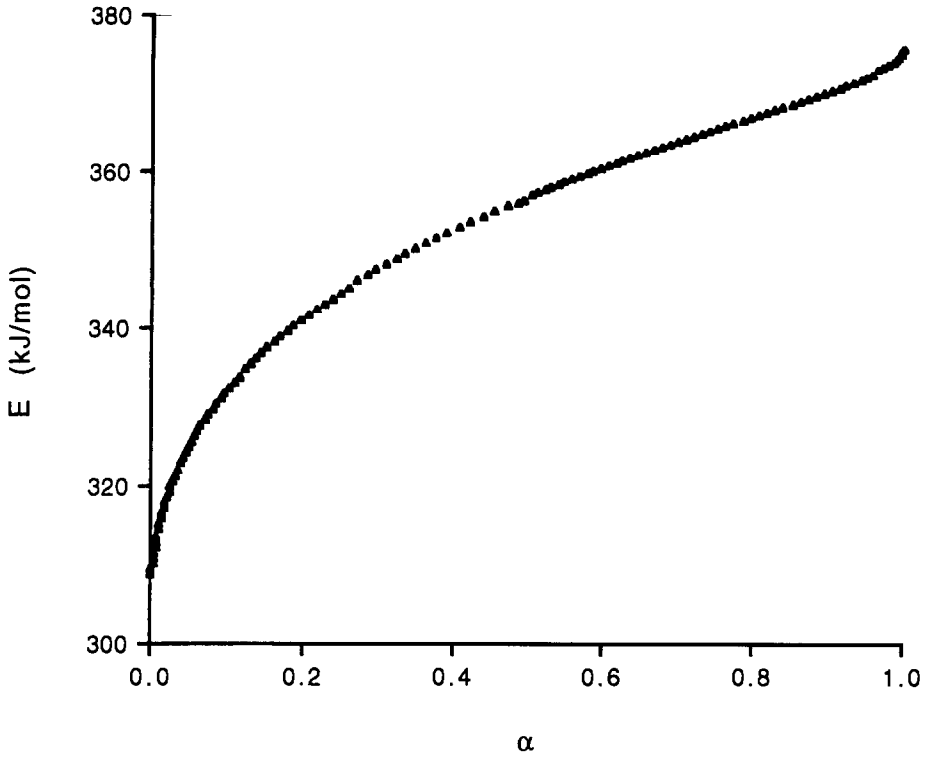

Fig. 9. Plot of E against α taken from the mid-point of the ΔT increment.

where ΔT is $(T_2 - T_1)$. This will give the value of E at the midpoint of ΔT as

$$E = \frac{m(\ln T_2 - \ln T_1) R T_1 T_2}{\Delta T} \tag{22}$$

This method can be used to detect changes in E and note its dependence on α and/or temperature. The method is simply to take the value of ΔT as small increments scanning the entire reaction temperature range. The possible variation in E can then be plotted against the corresponding value of α or T taken from the mid-point of the ΔT increment in each case, as shown in Figs. 8 and 9, respectively.

It is shown that although E is dependent on both α and temperature, the relationship is a linear one with temperature. Therefore, it is believed that the activation energy obtained from the above-mentioned methods should be a mean value for E over the reaction temperature region.

References

[1] E. Koch, Non-Isothernal Reaction Analysis, Academic Press, London, 1977, p. 44.
[2] J.J. Hood, Phil. Mag., 6 (1978) 731; 20 (1885) 323.
[3] S. Arrhenius, Z. Phys., 4 (1889) 226.

[4] A.V. Harcourt and W. Esson, Phil. Trans. R. Soc. London Ser A, 186 (1995) 187; 212 (1913) 187.
[5] M.E. Brown, D. Dollimore and A.K. Galway, in C.H. Bamford and C.F.H. Tipper (Eds.), Comprehensive Chemical Kinetics, Vol. 22, Reactions in the Solid State, Elsevier, Amsterdam, 1980, 340 pp.
[6] D. Dollimore, G.R. Heal and R.W. Krupay, Thermochim. Acta, 24 (2978) 293.
[7] R. Sh-Mikhail, D. Dollimore, A.M. Kamel and N.R. El-Nazer, J. Appl. Chem. Biotechnol, 23 (1973) 419.
[8] D. Dollimore and P.F. Rodgers, Thermochim. Acta, 30 (1979) 273.
[9] J. Sestak, Thermochim. Acta, 3 (1971) 150.
[10] C.D. Doyle, J. Appl. Polym. Sci., 5 (1961) 285; 6 (1962) 639.
[11] J. Zsako, J. Therm. Anal., 2 (1970) 141, 459.
[12] G. Gyulai and E.J. Greenbau, Thermochim. Acta, 6 (1973) 239.
[13] D. Dollimore, T.A. Evans, Y.F. Lee and F.E. Wilburn, Thermochim. Acta, 188 (1991) 77; 198 (1992) 249.
[14] D. Dollimore, T.A. Evans, Y.F. Lee and F.E. Wilburn, Thermochim. Acta, 196 (1992) 255.
[15] D. Dollimore, J. Therm. Anal., 38 (1992) 111.
[16] D. Dollimore, Thermochim. Acta, 203 (1992) 7.
[17] D. Chen, X. Gao and D. Dollimore, Anal. Instrum., 20 (1992) 137.
[18] S. Gao, D. Chen and D. Dollimore, Thermochim. Acta, 223 (1993) 75.
[19] A.M. Ginstling and B.I. Brounshtein, Zh. Prikl. Khim., 23 (1950) 1327.
[20] M. Brown, D. Dollimore and A.K. Galwey, in C.H. Bamford and C.F.H. Tipper (Eds.), Comprehensive Chemical Kinetics, Vol. 22, Elsevier, Amsterdam, 1980, Chapt. 3, p. 41.
[21] P.W.M. Jacobs and F.C. Tompkins, in W.E. Garner (Ed.), Chemistry of Solid State, Butterworths, London, 1955, Chapt. 7, p. 184.
[22] P.A.W. Haul and L.H. Stein, Trans. Faraday Soc., 51 (1955) 1280.